Chemical Engineering Journal 327 (2017) 1021–1032

Contents lists available at ScienceDirect

Chemical Engineering Journal

journal homepage: www.elsevier.com/locate/cej

Investigating the effects of heat activated persulfate on the degradation of furfural, a component of hydraulic fracturing fluid chemical additives

Katherine E. Manz, Kimberly E. Carter *

University of Tennessee/Oak Ridge National Laboratory, Bredesen Center, University of Tennessee, Knoxville, TN 37996, USA
Department of Civil and Environmental Engineering, University of Tennessee, Knoxville, TN 37996, USA

HIGHLIGHTS

- Degraded furfural using persulfate activated through heat, acidic pH, and iron.
- Furfural removal achieved with hydraulic fracturing chemical additives present.
- Reaction by-products and potential degradation pathways identified.

ARTICLE INFO

Article history:
Received 22 March 2017
Received in revised form 16 June 2017
Accepted 28 June 2017
Available online 29 June 2017

Keywords:
Furfural
3-Furaldehyde
Heat-activated persulfate
Oxidation
Fe (III)
Hydraulic fracturing chemical additives
Breaking agents

ABSTRACT

Improper well casings and produced water handling can lead to hydraulic fracturing fluid migration and groundwater pollution. Interactions among the chemical components can cause compositional changes in hydraulic fracturing fluids. This study focuses on degradation or transformations of 3-furfuraldehyde (or furfural) by activated-persulfate oxidation, two chemicals reported in hydraulic fracturing additives. As hydraulic fracturing conditions may be conducive to persulfate activation, the degradation of furfural was examined using elevated temperatures, varying persulfate dosing and Fe (III) concentration, initial pH, and the presence of other chemical additives (e.g., a gelling agent and an enzyme breaking agent).

Experiments showed furfural degradation using activated persulfate followed pseudo-first order kinetics with respect to the furfural concentration. Impacts of pH and ferric sulfate concentrations were investigated at different temperatures and the results were fit to the Arrhenius model to establish the activation energy. Decreasing the pH to 2.54 caused an increase in the furfural removal. The addition of ferric sulfate to solutions with pH 5.4 had no impact on the activation energy of furfural oxidation, which was 107 kJ mol^{-1}, while decreasing the pH to 2.54 allowed for the activation energy to decrease to 75 kJ mol^{-1}. Quenching with methanol and tert-butyl alcohol indicated significant hydroxyl radical contributions to furfural degradation compared to sulfate radicals during thermal persulfate activation in the presence of iron and acidic conditions. Furthermore, furfural degradation was monitored in the presence of other hydraulic fracturing chemical additives establishing furfural degradation does not occur as rapidly. However, furfural does still degrade in this matrix and this indicates that persulfate may break down other chemicals in hydraulic fracturing fluids more preferentially than the target gelling agent.

1. Introduction

Hydraulic fracturing, along with horizontal drilling, has permitted economical natural gas extraction from shale reserves [1,2]. The hydraulic fracturing process utilizes chemical additives, water, and sand at high pressures to produce fractures in the shale and stimulate the recovery of natural gas [3,4]. The chemical additives have various purposes (e.g., friction reducers, biocides, gelling agents and breaking agents) and contain a myriad of chemical compounds that are environmental concerns including methanol, ethoxylated surfactants, and formaldehyde [5–7]. Much of the current hydraulic fracturing research focuses on identifying chemical components of hydraulic fracturing fluids [6,8–11]. In the U.S. Environmental Protection Agency's (EPA) 2015 "Draft Assessment

* Corresponding author at: Department of Civil and Environmental Engineering, University of Tennessee, Knoxville, TN 37996, USA.
E-mail address: kcarte46@utk.edu (K.E. Carter).

http://dx.doi.org/10.1016/j.cej.2017.06.168
1385-8947/

of the Potential Impacts of Hydraulic Fracturing for Oil and Gas on Drinking Water Resources," transformation processes are considered important to understanding how hydraulic fracturing can affect the environment [12,13]. Currently, little is known about chemical additive transformation in hydraulic fracturing. Only recently have researchers begun to study chemical additive and shale transformation in abiotic and biotic conditions [13,14]. These studies have shown that chemical transformations do occur under hydraulic fracturing conditions, potentially causing more harmful or persistent byproducts that pose severe human health and environmental risks. However, the use of strong oxidizers, such as sodium persulfate, have not yet been considered in the research shift to transformation studies. Oxidizers likely play a strong role in chemical additive transformation, especially if they react with other constituents rather than the gelling agent they were intended to target.

Hydraulic fracturing companies use sodium persulfate as a "delayed" breaking agent and are used to decompose the gelling agents [15]. Persulfate salts are also used for contaminated groundwater remediation through *in situ* chemical oxidation (ISCO) because they do not decay rapidly or harm native microorganisms [16]. Of the commercially available persulfate salts (ammonium, sodium, and potassium), sodium persulfate has the greatest solubility (73 g/100 g H_2O at 25 °C) and is the most stable at 25 °C, making it the most preferable for hydraulic fracturing companies [17]. While the concentration of sodium persulfate used in fracturing depends on the conditions of the formation, site location, and hydraulic fracturing, concentrations as low as 0.125 mmol L^{-1} up to as much as 47 mmol L^{-1} have been reported [18–20].

Persulfate possesses an oxidation potential (E^0) of 2.01 V; however, once activated, it produces strong oxidizing sulfate radicals (E^0 = 2.7 V) as seen in reactions 1, 2, and 3 [21–23]. Persulfate activation occurs through electron transfer from transition metals such as iron, cobalt, or manganese, as well as through the use of heat, ultraviolet (UV) light, acidic conditions, or a combination of these activators [16,23–27]. Persulfate activation has also been shown to occurring using the oxidized form, Me^{n+1}, of the transition metals manganese and iron, as shown in Reaction (4) [28–30]. When Fe (III) is present, a persulfate radical and Fe (II) are generated. The Fe (II) produced may further react with persulfate anions as shown in Reaction (2), enabling further organic contaminant removal. Organic compounds may also participate in iron recycling, reducing Fe (III) to Fe (II) as shown in Reaction (5) [31].

$$S_2O_8^{2-} \xrightarrow{heat\ or\ UV} 2SO_4^{\cdot-} \qquad k = 1.1 * 10^{10} M^{-1}s^{-1} \tag{1}$$

$$S_2O_8^{2-} + Me^{n+} \rightarrow SO_4^{\cdot-} + Me^{n+1} + SO_4^{2-} \qquad k = 20 M^{-1}s^{-1} \text{ for } Fe^{2+} \tag{2}$$

$$SO_4^{\cdot-} + H_2O \rightarrow SO_4^{2-} + OH^{\cdot} + H^+ \qquad k = 660\ s^{-1} \tag{3}$$

$$S_2O_8^{2-} + Me^{n+1} \rightarrow S_2O_8^{\cdot-} + Me^{n+} \tag{4}$$

$$R + Fe^{3+} \rightarrow Fe^{2+} + products \tag{5}$$

The conditions faced in hydraulic fracturing provide an adequate environment for persulfate activation. Over the course of a fracture, downhole temperatures may exceed 140 °C [32]. Hydrochloric acid, one of the most common additives used in hydraulic fracturing [33], may influence the extent of persulfate reactions. Concentrations of hydrochloric acid used may range from 0.012% to 15% of the total water [34–37], but is reported as 0.07% by FracFocus.org [38–40]. The dissolved iron content in hydraulic fracturing fluids ranges between 0.1 and 222 mg L^{-1}, while total iron can range between 2.6 and 321 mg L^{-1} [41]. A previous study regarding the quality of flowback water determined the total iron content as 16 mg L^{-1}, while Fe^{2+} content was below the detection limits of the study (0.2 mg L^{-1}) [42]. This suggested that the predominant oxidation state of iron was either Fe (III) or Fe(0) for the flowback fluid samples from this study [42]. The presence of Fe (III) likely arises from the fluid's interaction with shale rock, as shale contains various iron oxides (e.g., hematite (Fe_2O_3)) [43–46]. In addition, ferric sulfate has also been found in at least 7 different chemical products added by hydraulic fracturing companies [47]. The potential combination of persulfate activators and conditions present in hydraulic fracturing fluids of the shale formation may provide an environment for the breakdown of chemical additives other than the target gelling agent. Therefore, the objective of this research is to investigate the reaction of persulfate exposed to elevated temperatures, pH changes, and the chemical additives in hydraulic fracturing fluids and to determine if these conditions are conducive to persulfate transformation of organic contaminants in produced waters [3,6,32,47,48].

This study is to systematically determine how a hydraulic fracturing chemical additive interacts with persulfate in different conditions and ultimately investigate if persulfate preferentially attacks the additive or the target gelling agent. Furfural, or 3-furaldehyde, was identified as a contaminant of interest in the components of a hydraulic fracturing enzyme breaker and used to study hydraulic fracturing fluid interactions with sodium persulfate. In addition, furfural has also been used as a coating polymer for proppants in hydraulic fracturing fluids [47,49,50] because it is highly resistant to heat, acid, and water [51]. Furfural's interactions with sodium persulfate are investigated in the presence of different activators which may be encountered during hydraulic fracturing and include heat (20 to 60 °C), ferric sulfate, and pH variations. Oxidation reaction by-products were determined using gas chromatography mass spectrometry (GC/MS). Finally, this study goes a step further by examining the impact other organic compounds have on furfural degradation when present in hydraulic fracturing fluids by comparing reaction kinetics when an enzyme breaking agent and a gelling agent are present in solution. Insight into the interactions between furfural and sodium persulfate enables the understanding of how the oxidizing breaking agent used in hydraulic fracturing fluids impact the quality and treatability of the flowback/produced water returning to the surface.

2. Materials and methods

2.1. Chemicals

All solutions were prepared using deionized water from a Milli-Q Plus water purification system (Darmstadt, Germany). Furfural was purchased from Sigma Aldrich (St. Louis, MO 63103). Optima grade hexane, methylene chloride, ethyl acetate, methanol, tert-butanol (TBA) and toluene were purchased from Fisher Scientific (Pittsburgh, PA 15275, USA). Inorganic salts, including sodium persulfate (>98%), sodium bicarbonate (>99%), and potassium iodide (>99%), were purchased from Fisher Scientific (Pittsburgh, PA 15275, USA). pH was adjusted with hydrochloric acid (35–38%) and sodium hydroxide (>97%), which were obtained from Fisher Scientific (Pittsburgh, PA 15275, USA). LEB-10X, an enzyme breaker, and WGA, a gelling agent, were obtained from Weatherford International (Houston, Texas, USA).

2.2. Experimental procedures

2.2.1. Batch heat-activated oxidation experiments

Furfural solutions were prepared 24 h prior to starting the experiment and mixed using a magnetic stir bar. The initial

concentration of furfural was 120 mg L^{-1}. In experiments containing quenchers or hydraulic fracturing chemical additives, the additional organics were added to the furfural solution and mixed for 12 h prior to the start of the experiment. Methanol and TBA were used to quench the reactions with the activated-persulfate. The methanol and TBA were added to solution using a molar ratio ranging from 1:10 to 1:100 furfural to quencher, depending on the amount required to quench the furfural degradation reaction.

In order to examine how fracturing chemicals impact the degradation of furfural, LEB-10X and WGA were added in concentrations typically observed in hydraulic fracturing treatments, as indicated by the chemical supplier [52]. For LEB-10X, this concentration was 0.025 gallons per 1000 gallons of water and for WGA this concentration was 25 pounds per 1000 gallons of water. Solution pH was measured with a Fisher Scientific Accumet XL600 benchtop meter (Pittsburgh, PA 15275, USA) and adjusted to pH 2.54, 5.4, or 10.4 using sodium hydroxide or hydrochloric acid. Initially, hydrochloric acid was added so that the volume was equal to 0.07% of the total volume, as has been reported by in hydraulic fracturing companies [38–40]. This resulted in a final pH of 2.54, therefore all acidic solutions were adjusted to this initial pH.

All experiments were carried out in triplicate using 125 mL capped amber borosilicate VOC (volatile organic carbon) bottles closed with Teflon-lined screw caps containing 100 mL of the furfural solution. The jars were set in a shaking water bath at 20, 30, 40, 55, and 60 °C at least 12 h prior to the addition of sodium persulfate (New Brunswick Scientific Co, Inc, Model G76, Edison, NJ USA). Sodium persulfate stock solutions (1050 mM) were prepared 1 h prior to the reaction. The reaction was initiated by spiking each amber jar with the appropriate volume of sodium persulfate solution to a final persulfate concentration of 0.6, 5, 10, 15, or 21 mmol L^{-1}. Each experiment was carried out for a minimum of 8 h, the approximate length of a fracture. Experimental controls without persulfate were prepared in the same manner to establish furfural losses not caused by the activated-persulfate oxidation. A 4.5 mL sample was collected at various time points throughout the 8-h experiment and placed in an Eppendorf centrifuge tube. The tubes were placed in an ice bath to quench the oxidation reaction caused by residual persulfate and analyzed within 2 h of collection.

2.2.2. Furfural, total organic carbon, persulfate anion, and Fe (II) analysis

The furfural degradation matrix in each sample was measured using a UV/Vis spectrophotometer (Thermo Fisher Scientific, Model Evolution 600 Madison, WI 53711, US) at the maximum wavelength of 258 nm [53–55]. Samples were previously scanned to determine any interferences from compounds whose absorbance is 258 nm prior to the start of the experiments. Calibration curves were made using standards containing known furfural. Standard error (SE) of the data were represented by error bars in the Figures and was calculated using Eq. (1), where s is the sample standard deviation and n is the number of observations.

$$SE = \frac{s}{\sqrt{n}} \quad (1)$$

Total organic carbon (TOC) was determined using a TOC-LCSH/CSN series standalone analyzer equipped with an ASI autosampler (Shimadzu, Kyoto, Japan). TOC standards were made using a known amount of furfural in water. Samples were run in triplicate to ensure repeatability of the measurements. TOC was determined using the difference between the total carbon (TC) and inorganic carbon (IC) concentrations.

Persulfate anion measurements were performed using a modified spectrophotometric/iodometric methods [56]. A solution of 166 g L^{-1} potassium iodide and 12 g L^{-1} sodium bicarbonate were prepared in water and placed on a stir plate until all components dissolved. A 5-mL aliquot of this solution was added to a separate vial along with 25 to 100 μl of sample (depending on the expected persulfate concentration) and allowed to react for 20 min. The resulting mixture was measured using a UV/Vis spectrophotometer (Thermo Fisher Scientific, Model Evolution 600 Madison, WI 53711, US) at the maximum wavelength of 352 nm. Standards were prepared in the same manner, by pipetting solutions containing known concentrations of sodium persulfate stock solution into 5 mL aliquots of the potassium iodide-sodium bicarbonate solution.

Fe (II) was analyzed colorimetrically using Hach® Ferrous Iron reagent powder pillows according to Hach® Method 8146 (Hach Company, Loveland, CO 80539). The resulting complex Fe (II) forms with 1,10-phenanthroline was measured at the maximum wavelength of 510 nm using a UV/Vis spectrophotometer (Thermo Fisher Scientific, Model Evolution 600 Madison, WI 53711, US).

2.2.3. Reaction byproducts analysis

Samples were extracted using liquid-liquid extraction previously described technique [11]. Briefly, the liquid-liquid extractions were performed with 3 mL of sample and a total of 3 mL of hexane, dichloromethane, toluene, or ethyl acetate. The sample was pipetted into scintillation vials, 1 mL of organic solvent was added, the vials were vortexed for 30 s using a 115 V Mini Vortex Mixer (Fisher Scientific, Pittsburgh, PA 15275, USA). The organic phase was separated from the aqueous phase using a 6-mL polypropylene syringe (Fisher Scientific, Pittsburgh, PA 15275, USA). The procedure was repeated 3 times, for a total of 3 mL organic solvent.

Mass spectra were obtained using an Agilent 7890B gas chromatograph equipped with a DB-1 capillary column (30 m × 0.25 mm inner diameter × 0.25 μm film thickness) interfaced to a 5977 A Mass Selective Detector (MSD) (Santa Clara, CA 95051, USA). Ultra-high purity helium purchased from Airgas Corporation was used as the carrier gas and maintained at 1.5 mL min^{-1} (Knoxville, TN 37921, USA). The GC was operated in splitless mode with an injection volume of 2 μL. The initial temperature of the GC was 40 °C and was held for 2 min. The temperature ramp was 2.5 °C/min to 100 °C, which was held for 2 min. For samples with LEB-10X, the temperature ramp was extended to 200 °C. Using the gas chromatograms and the NIST11 mass spectral library database, the different byproducts formed during the activated-persulfate oxidation furfural were identified.

3. Results and discussion

3.1. Temperature Effects

Experiments were performed at temperatures of 20, 30, 40, 55, and 60 °C to examine the influence thermally-activated persulfate has on the removal of furfural. Fig. 1 displays the decrease in furfural concentration from 30 to 60 °C using (a) pH 2.54 and (b) pH 5.4 and an initial sodium persulfate dose of 21 mmol L^{-1}. Fig. S1 of the Supplementary Materials displays the furfural degradation under the same conditions at 20 °C as persulfate activates much slower at this temperature. The data shows the furfural concentration decreased more rapidly at the higher temperatures, which is an expected result from previous studies using thermally-activated persulfate [21,57]. Control experiments were performed under similar conditions without persulfate at 20 °C to confirm the furfural removal from solution was due to thermally-activated persulfate degradation. Fig. S2 shows the change in furfural concentration as a function of time at 20 °C without persulfate. As previous studies have shown, the furfural concentration

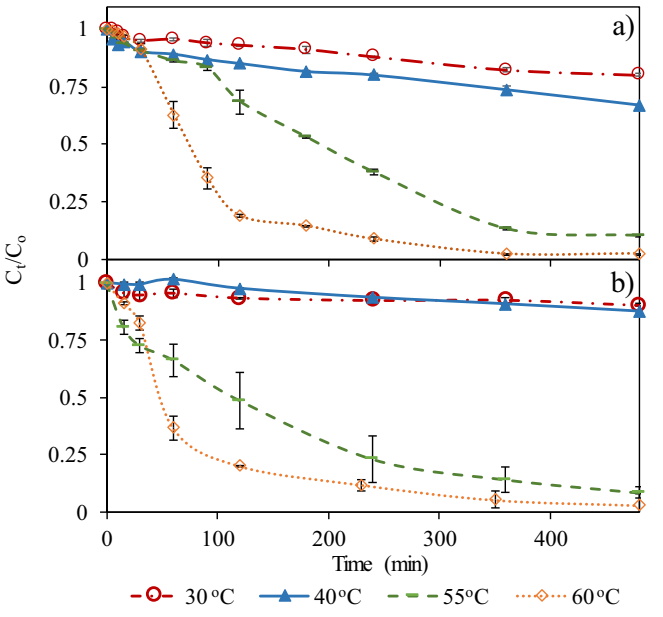

Fig. 1. Change in furfural concentration at 30, 40, 55, and 60 °C using an initial sodium persulfate dose of 21 mmol L^{-1} (ferric sulfate = 0 mg L^{-1}). Experiment were performed with an initial (a) pH 2.54 and (b) pH 5.4. Error bars represent standard error.

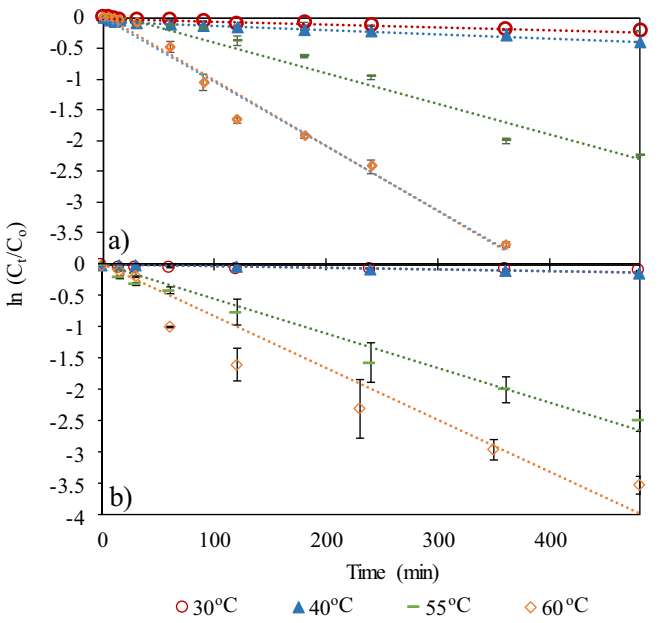

Fig. 2. Changes in furfural concentrations due to reactions with an initial sodium persulfate dose of 21 mmol L^{-1}. Experiments were performed using an initial (a) pH 2.54 and (b) pH 5.4 over the course of 480 min. Error bars represent standard error.

remained constant with elevated temperatures in the absence of persulfate [58], which is further confirmed in Fig. S2 where the concentration of furfural decreased by less than 20% after 450 h (7.5 days). This suggests that the volatilization and hydrolysis of furfural was very slow and had negligible impact on the removal of furfural compared to the experiments where persulfate was present.

The degradation of furfural appeared to decrease exponentially suggesting that pseudo-first order kinetics were involved. Therefore, pseudo-first order rate constants were determined over the temperature range tested using Eq. (2), where C is the furfural concentration (mole L^{-1}) at a specific time, t, and k_{obs} is the overall pseudo first-order rate constant (s^{-1}) and assuming the radical species produced ($SO_4^{\cdot-}$, $HO^{\cdot}$, etc.) were present in excess and that the loss of furfural was irreversible. Fig. 2 shows the linearized data using Eq. (2) from the temperature effect experiments at (a) pH 2.54 and (b) pH 5.4. Comparing reaction rates for pH 2.54 to pH 5.4 at 55 and 60 °C, little change occurred in furfural degradation rate as shown in the slope of the ln (C_o/C_t) versus time plots in Fig. 2a and b. The data also showed less furfural degradation occurred at 30 and 40 °C over the course of 8 h than at the elevated temperatures of 55 and 60 °C, indicating the temperature has a greater impact than the initial pH [59,60]. As elevated temperatures are present during a fracture, it is likely that the persulfate will rapidly degrade chemical additives found in the fracturing fluids including furfural.

$$ln\left(\frac{C}{C_o}\right) = k_{obs} * t \tag{2}$$

Table 1 summarizes the pseudo first-order rate constants for temperature dependency experiments and shows the furfural removal rate constants increased by 3 orders of magnitude from 20 °C to 60 °C. The observed increasing reaction rates with elevated temperatures further implies that the temperature plays a significant role in furfural removal with persulfate present. The persistence of furfural was assessed by determining the half-life of the compound using Eq. (3), where $t_{1/2}$ is the furfural half-life in seconds. The half-life data obtained for all temperature conditions are also summarized in Table 1. The data show that the half-life decreased when the temperature increased from 20 °C to 60 °C. The half-lives at each temperature were less than the hydrolysis half-life of furfural in DI water with no persulfate present, which was determined to be 84.7 days ± 0.34 at room temperature (Fig. S2). The decreasing half-life with persulfate present indicates persulfate, sulfate, or hydroxyl radicals play a role in the removal of the furfural when the temperature is elevated.

$$t_{\frac{1}{2}} = \frac{\ln(2)}{k_{obs}} \tag{3}$$

Fig. 3 shows the change in furfural concentration with 23.3 mg L^{-1} ferric sulfate at (a) pH 2.54 and (b) pH 5.4, with temperatures ranging from 30 to 60 °C . The full-time scale of furfural degradation tested at 20, 30 and 40 °C are displayed in Figs. S3–S5, respectively (Supplementary Materials). As shown in these Figures, less furfural degradation was achieved using temperatures of 20, 30 and 40 °C during the 8 h experiments. At 20 °C, decreasing the initial pH resulted in increasing furfural degradation rates as shown in Fig. S3. Again, the experiments performed at 20 °C showed the furfural degradation progressed much slower than the experiments performed at the higher temperatures [21,57]. Though the degradation rate is slower at the lower temperatures in the beginning of each experiment, Fig. 3a shows there was little impact on the final furfural removal with respect to the temperature when the initial pH of 2.54 was used, and almost complete furfural removal was achieved within the 8-h experiment. Fig. 3b shows that increasing the pH from 2.54 to 5.4 had a detrimental impact on the furfural degradation at lower temperatures as the reactions were much slower, while degradation appeared to be similar for the higher temperatures regardless of pH.

The observed reaction rate constants, k_{obs}, for the data from Fig. 3 are also listed in Table 1. Compared to the data in Fig. 1, where no ferric sulfate is present, the k_{obs} from Fig. 3 suggests that pH has little impact on thermally-activated persulfate decomposition of furfural. However, when ferric sulfate is present in solution, the pH appears to influence the furfural degradation as shown in Fig. 3. This may be due to the variation in Fe states and complexes

Table 1
Pseudo first-order reaction rate constants for furfural oxidation via activated persulfate as temperature is increased.

$[Na_2S_2O_8]_i$ (mM)	$[Fe_2(SO_4)_3]_i$ (mg L^{-1})	pH	T (°C)	k_{obs} (s^{-1})	$t_{1/2}$ (d)	R^2
21	0	5.4	20	8.79×10^{-7}	9.13	0.95
21	0	5.4	30	3.53×10^{-6}	2.27	0.91
21	0	5.4	40	6.53×10^{-6}	1.23	0.93
21	0	5.4	55	1.10×10^{-4}	0.0729	0.98
21	0	5.4	60	1.49×10^{-4}	0.0538	0.94
21	23.3	5.4	20	9.46×10^{-7}	8.48	0.93
21	23.3	5.4	30	5.20×10^{-6}	1.54	0.97
21	23.3	5.4	40	3.25×10^{-5}	0.247	0.96
21	23.3	5.4	55	1.59×10^{-4}	0.0505	0.91
21	23.3	5.4	60	1.62×10^{-4}	0.0496	0.93
21	0	2.54	20	3.29×10^{-6}	2.44	0.96
21	0	2.54	30	1.02×10^{-5}	0.788	0.92
21	0	2.54	45	3.19×10^{-5}	0.251	0.89
21	0	2.54	55	7.79×10^{-5}	0.103	0.96
21	0	2.54	60	1.52×10^{-4}	0.0528	0.95
21	23.3	2.54	20	1.73×10^{-5}	0.464	0.91
21	23.3	2.54	30	4.28×10^{-5}	0.187	0.89
21	23.3	2.54	45	1.73×10^{-4}	0.0464	0.95
21	23.3	2.54	55	4.47×10^{-4}	0.0179	0.93
21	23.3	2.54	60	6.89×10^{-4}	0.0116	0.98

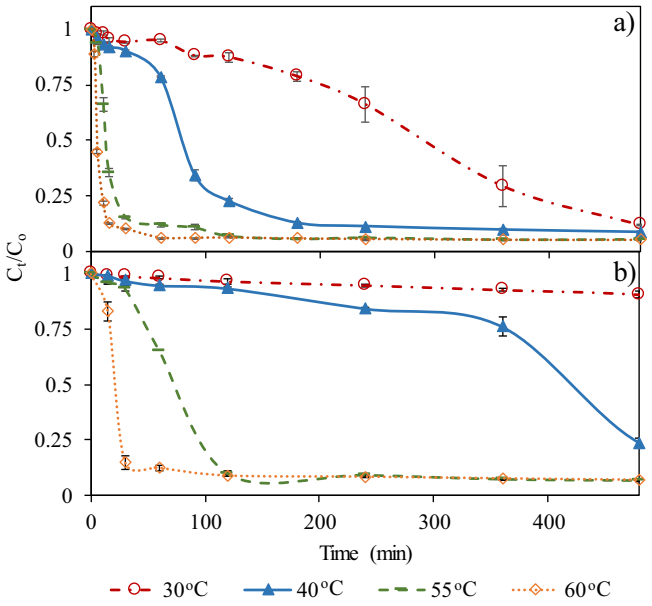

Fig. 3. Changes in furfural concentrations due to reactions with an initial sodium persulfate dose of 21 mmol L^{-1} and a ferric sulfate dose of 23.3 mg L^{-1}. Experiments were performed using an initial pH of (a) 2.54 and (b) 5.4 over the course of 480 min. Error bars represent standard error.

that form at the pHs tested that promote persulfate activation resulting in faster furfural breakdown [61]. Upon further investigation, in the absence of thermal activation, Fe (III) was not determined to be converted to Fe (II) in the presence of persulfate nor furfural alone at pH 5.4. Fig. S6 shows the furfural, Fe (II), and persulfate concentrations in the reactions of furfural and Fe (III), persulfate and Fe (III), and furfural with both persulfate and Fe (III) at 20 °C (initial pH 5.4, 23.3 mg L^{-1} ferric sulfate and 21 mmol L^{-1} persulfate when used). Iron alone did not degrade furfural. This suggest that no furfural-iron complex is forming, which is further verified by the measurements of Fe (II) shown in Fig. S6b because Fe (II) remains at the detection limit. Chelation between furfural and Fe (III) did not occur, as increasing Fe (II) concentrations were not detected in the experiments. Fe (II) only formed when the combination of all three species (furfural, persulfate, and Fe (III)) was present. Therefore, Fe (III) recycling likely does not occur by persulfate or organic furfural alone at room temperature, as suggested by Reactions (4) and (5). Rather, a synergistic reaction occurs between all three at room temperature. Thus, the mechanism of furfural degradation without thermal activation (20 °C) by persulfate/Fe (III) warrants further investigation.

The activation energies for the data shown in Figs. S7 and S8 in the Supplementary Materials were determined by plotting the k_{obs} versus the inverse of the absolute temperature as and using the Arrhenius Equation (Eq. (4)), where E_a is the activation energy (J mol^{-1}), A is the frequency factor (s^{-1}), R is the universal gas constant (J K^{-1} mol^{-1}), and T is absolute temperature (K). The activation energy (E_a) of furfural oxidation was established at both pH 2.54 and 5.4 by taking the slope of each line. The activation energies for these experiments are summarized in Table 2 when ferric sulfate was and was not present in the solution. The activation energy was 107.3 kJ mol^{-1} (R^2=0.93) for furfural oxidation using 21 mmol L^{-1} persulfate, without ferric sulfate at pH 5.4. In the presence of 23.3 mg L^{-1} ferric sulfate at pH 5.4, the activation energy of furfural oxidation was 107.6 kJ mol^{-1} (R^2=0.99). When the initial was pH 2.54, the activation energy was 74.3 kJ mol^{-1} (R^2=0.99) without ferric sulfate and 75.2 kJ mol^{-1} (R^2=0.99) with 23.3 mg L^{-1} ferric sulfate. As illustrated in Supplementary Materials Fig. S9, the presence of ferric sulfate did not affect the activation energy. However, the differences in activation energy based on the initial pH suggests that decreasing the pH significantly lowers the energy barrier for furfural degradation to occur and that pH may be a stronger activator than Fe (III) for furfural degradation by activated persulfate oxidation [31,61].

$$\ln k_{obs} = \ln A - \frac{E_a}{RT} \quad (4)$$

3.2. Effect of pH

As observed in Supplementary Materials Fig. S9, the activation energy is impacted by the solution pH. Therefore, further effects of pH (2.54, 5.4, 10.4) on furfural degradation without the presence of ferric sulfate for sodium persulfate concentrations of 5, 10, 15 mmol L^{-1} was investigated. pH 10.4 was tested, which has been shown to activate persulfate [62], but is not customarily used in hydraulic fracturing well treatments. However, this pH may occur through reactions with the shale rock [35]. Control experiments were performed to evaluate coagulation effects on furfural with

Table 2
Arrhenius parameters for furfural removal.

$[Fe_2(SO_4)_3]_i$ (mg L^{-1})	pH	E_a (kJ mol^{-1})	A (s^{-1})	R^2
0	5.4	107.3	9.52×10^{12}	0.93
23.3	5.4	107.6	1.83×10^{13}	0.99
0	2.54	74.3	5.78×10^{7}	0.99
23.3	2.54	75.2	4.07×10^{8}	0.99

ferric sulfate. The data is displayed in Fig. S10 in the Supplementary Materials and data show that no coagulation or complexing took place over the 8-h time period at all pHs tested in this study. The decrease in furfural concentration over time for each pH and sodium persulfate dose is shown in Supplementary Materials Fig. S11a-f and the pseudo first-order reaction rate constants are displayed in Table 3. Comparing all the persulfate concentrations tested, the highest degradation rate constant was observed at pH 2.54. As illustrated in Supplementary Materials Fig. S12, the rate constant was higher in basic conditions than at neutral pHs. However, the reaction rate constant at basic pH (10.4) was less than the reaction rate constant of the solution with the acidic pH (2.54), which is similar to the pH encountered during well treatment with hydraulic fracturing. This suggests that during the fracturing of a well, the acidic pHs used in the industry may be capable of aiding in the oxidation of furfural or other compounds using heat activated persulfate [22,23].

Supplementary Materials Figs. S13 and S14 show the pH profiles of the 55 °C experiments with 5, 10, and 15 mmol L^{-1} sodium persulfate dosing and when ferric sulfate concentration was 0 and 23.3 mg L^{-1}, respectively. In both Figures, a) displays when the initial was pH 2.54 and b) displays when the initial pH was 5.4. Independent of iron concentration, as the reaction proceeds pH decreases. As the oxidation reactions proceed at 55 °C with 23.3 mg L^{-1} ferric sulfate added, the pH decreases from 2.54 to 2.17 with an initial sodium persulfate dose of 10 mmol L^{-1} and to 1.99 with an initial dose of 15 mmol L^{-1} after 480 min. Without ferric sulfate, the pH decreases from 2.54 to 2.08 after 480 min with sodium persulfate doses of 10 and 15 mmol L^{-1}. After 1400 min, the final pH is 1.96 for both sodium persulfate doses. The decreasing pH exhibited is even more pronounced when the initial pH is 5.4, as pH decreases to 2.82 with an initial sodium persulfate dose of 10 mmol L^{-1} and to 2.43 with an initial dose of 15 mmol L^{-1} when iron is present after 480 min. More pronounced pH decrease is also observed when no ferric sulfate is present in solution; the lowest pH of 2.17 is reached by 480 min and does not decrease any more as the reaction proceeds to 1400 min.

While Reaction (1) will occur at acidic and neutral pHs using heat activated persulfate, the decrease in pH gives evidence that Reaction (3) may also occur during furfural degradation because hydrogen ions are released from the furfural molecule into water as the reaction proceeds, further decreasing solution pH. Additionally, the persulfate anion can breakdown into the sulfate radical in acidic conditions through Reactions (6) and (7), again, further decreasing the solution pH [59,63]. Regardless, the higher observed pseudo first-order reaction rate constant at acidic pH indicates that the probability for radical-to-contaminant reactions is higher and is likely due to increased production of sulfate or hydroxyl radicals. In hydraulic fracturing, increased production of radicals may decrease overall chemical additive removal efficiency because very fast radical-to-radical reactions may be favored over radical-to-additive interactions [23,64]. When this occurs, the persulfate source is depleted without removing a portion of the chemical additives.

$$S_2O_8^{2-} + H^+ \rightarrow HS_2O_8^- \quad (6)$$

$$HS_2O_8^- \rightarrow SO_4^{\cdot-} + SO_4^{2-} + H^+ \quad (7)$$

3.3. Effects of initial persulfate concentration

Experiments were performed with 0.6, 5, 10, 15, and 21 mM persulfate, at 55 °C and pH of 5.4 to establish the impacts persulfate concentration has on furfural removal. pH 5.4 was used to systematically determine the impacts of persulfate dose without any added factors. Fig. 4 shows the results of this experiment with both 0 mg L^{-1} and 23.3 mg L^{-1} of ferric sulfate. When 23.3 mg L^{-1} ferric sulfate was present in solution, >90% furfural removal was achieved after 120 min with initial sodium persulfate doses of 10, 15, and 21 mM. Without the addition of ferric sulfate, the greatest furfural removal was 97%, but was only obtained using a persulfate dose of 21 mM and the reaction time was extended to 480 min. While overall, higher initial persulfate concentrations led to higher furfural degradation rates when no ferric sulfate was in solution, in the presence of ferric sulfate there appeared to be a maximum persulfate concentration required for furfural removal. Table 4 lists the pseudo first-order rate constants for

Table 3
Pseudo first-order reaction rate constants for furfural oxidation via activated persulfate as an effect of pH change.

$[Na_2S_2O_8]_i$ (mM)	$[Fe_2(SO_4)_3]_i$ (mg L^{-1})	pH	T (°C)	k_{obs} (s^{-1})	$t_{1/2}$ (d)	R^2
5	0	2.54	55	7.26×10^{-5}	0.110	0.97
5	0	5.4	55	1.58×10^{-5}	0.508	0.97
5	0	10.4	55	4.95×10^{-5}	0.162	0.95
10	0	2.54	55	8.87×10^{-5}	0.0904	0.94
10	0	5.4	55	3.69×10^{-5}	0.218	0.98
10	0	10.4	55	4.92×10^{-5}	0.163	0.95
15	0	2.54	55	9.18×10^{-5}	0.0874	0.95
15	0	5.4	55	6.67×10^{-5}	0.120	0.97
15	0	10.4	55	9.07×10^{-5}	0.0883	0.98
5	23.3	2.54	55	3.21×10^{-4}	0.0250	0.95
5	23.3	5.4	55	8.21×10^{-5}	0.0979	0.98
10	23.3	2.54	55	3.93×10^{-4}	0.0204	0.94
10	23.3	5.4	55	1.44×10^{-4}	0.0558	0.94
15	23.3	2.54	55	4.11×10^{-4}	0.0195	0.96
15	23.3	5.4	55	1.56×10^{-4}	0.0514	0.96

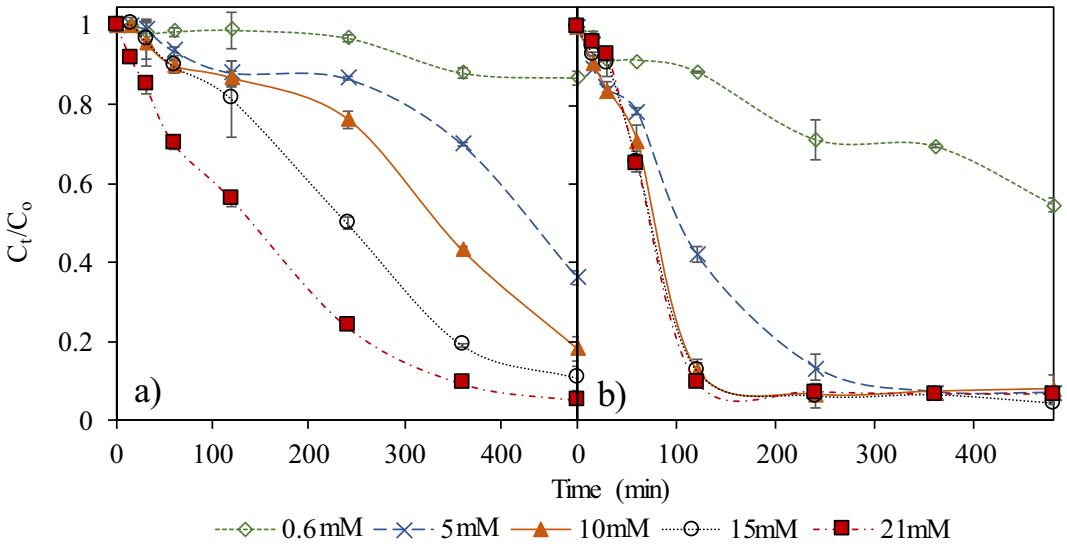

Fig. 4. Effect of persulfate dose on the furfural concentration at 55 °C and pH 5.4 with (a) 0 mg L^{-1} ferric sulfate and (b) 23.3 mg L^{-1} ferric sulfate. Faster decreasing concentrations were observed with ferric sulfate in solution. Error bars represent standard error.

Table 4
Pseudo first-order reaction rate constants for furfural oxidation as the sodium persulfate dose is increased.

$[Na_2S_2O_8]_i$ (mM)	$[Fe_2(SO_4)_3]_i$ (mg L^{-1})	pH	T (°C)	k_{obs} (s^{-1})	$t_{1/2}$ (d)	R^2
0.6	0	5.4	55	5.24×10^{-6}	1.53	0.98
5	0	5.4	55	1.58×10^{-5}	0.508	0.97
10	0	5.4	55	3.96×10^{-5}	0.203	0.98
15	0	5.4	55	6.67×10^{-5}	0.120	0.97
21	0	5.4	55	1.10×10^{-4}	0.0729	0.98
0.6	23.3	5.4	55	2.01×10^{-5}	0.399	0.95
5	23.3	5.4	55	8.21×10^{-5}	0.0977	0.98
10	23.3	5.4	55	1.30×10^{-4}	0.0557	0.94
15	23.3	5.4	55	1.56×10^{-4}	0.0514	0.96
21	23.3	5.4	55	1.59×10^{-4}	0.0505	0.91

the data in Fig. 4. Supplementary Materials Fig. S15 shows the observed pseudo first-order rate constants versus the initial persulfate dosage with both 0 and 23.3 mg L^{-1} ferric sulfate. In both cases, the relationship between initial persulfate concentration and the pseudo first-order rate constant is linear (R^2=0.99 for the solution without ferric sulfate, R^2=0.96 for solutions with 23.3 mgL^{-1} ferric sulfate). The addition of ferric sulfate increases the furfural degradation rate between 10 to 30% depending on the persulfate dosage, thus aiding in the degradation of the compound.

The amounts of the persulfate anion left in solution as furfural removal proceeds is displayed in Supplementary Materials, Fig. S16a (55 °C pHs 2.54 and 5.4, 0 and 23.3 mg L^{-1} ferric sulfate). More persulfate is used in the first 5 min when iron is present at both pHs. However, the difference is much greater at pH 2.54 than at pH 5.4. At pH 5.4, 11.3 mmol L^{-1} persulfate (75% remaining) remains in solution when no iron is present and 9 mmol L^{-1} persulfate (60% remaining) remains when iron is present. At pH 2.54, 13.5 mmol L^{-1} persulfate (90% remaining) remains in solution when no iron is present and 6.6 mmol L^{-1} persulfate (44% remaining) remains when iron is present. This implies that iron present in the acidic hydraulic fracturing fluids will aid in the removal of different organic contaminants, but will also deplete the persulfate, requiring additional persulfate dosing.

The TOC remaining during furfural breakdown is displayed in Supplementary Materials, Fig. S16b (55 °C pHs 2.54 and 5.4, 0 and 23.3 mg L^{-1} ferric sulfate).The TOC removal was fastest in the presence of iron at pH 2.54 and also occurred to a greater extent than when there was no iron present suggesting less byproduct formation occurred under these conditions. At pH 5.4, the TOC removal was greater during the initial first 15 min when iron is present; however, after 60 min, the solution without iron achieves almost as much TOC removal as pH 2.54 with iron. TOC removal on 1400-min extended time-scale for reactions without ferric sulfate (55 °C, initial sodium persulfate dose = 15 mmol L^{-1}, pH = 2.54 and 5.4) are shown in Supplementary Materials Fig. S17. An observed 99% TOC removal was achieved after 23.1 h and 23.3 h of reaction time for pH 2.54 and pH 5.4, respectively, both without iron.

3.4. Effects of iron concentration

Fig. 5a shows the effect of varying ferric sulfate concentrations on furfural removal using a constant persulfate dose of 15 mM. Furfural removal was 95% after reacting with the persulfate and ferric sulfate concentrations of 5, 10 and 25 mg L^{-1} for 480 min. When 25 mg L^{-1} ferric sulfate was in solution, 95% furfural removal was achieved within 160 min, whereas decreasing the ferric sulfate concentration to 10 mg L^{-1} and 5 mg L^{-1} of ferric sulfate required 250 and 480 min, respectively, to achieve the same amount of removal. While using 25 mg L^{-1} of ferric sulfate allowed for 95% removal of the furfural, increasing the ferric sulfate concentration to 50 and 100 mg L^{-1} caused a decrease in the overall furfural removal. Fig. 5b shows the k_{obs} versus the ferric sulfate concentrations. Table 5 lists the observed pseudo first order rate

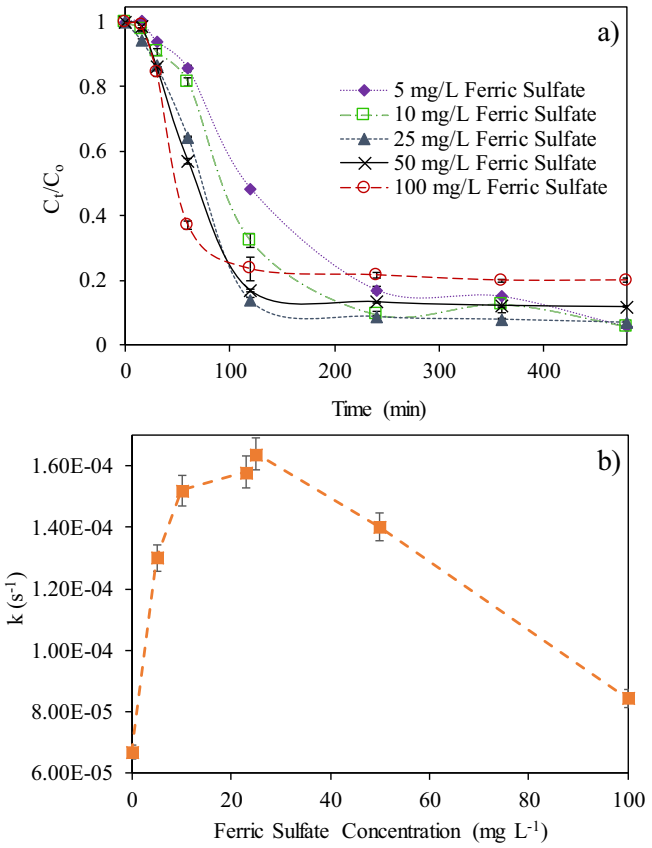

Fig. 5. (a) Effect of iron concentration on furfural degradation over time at 55 °C, pH 5.4, and an initial persulfate dose of 15 mM and (b) Observed reaction rate constants as a function of ferric sulfate concentrations are shown.

constants for these experiments, which gradually increased until the ferric sulfate concentration reached 25 mg L^{-1} ferric sulfate (k_{obs} = 1.65 × 10^{-4} s^{-1}). As shown in Fig. 5b, when the ferric sulfate concentrations were >25 mg L^{-1}, the pseudo first order reaction rate constant begins to decrease. This suggests a maximum ferric iron dose exists for furfural degradation. Concentrations above the maximum dose may cause the excess iron to scavenge or react with the persulfate faster than the formed radicals can attack the furfural, thus hindering the persulfate oxidation [65].

3.5. Identification of radicals via quenching

Experiments were carried out using methanol and TBA to determine the radical species that contributes to the furfural degradation [66–68]. Methanol has a reaction rate constant of 3.2 × 10^6 M^{-1} s^{-1} with sulfate radicals and 9.7 × 10^8 M^{-1} s^{-1} with hydroxyl radicals and has similar reactions with both radical species. TBA has a reaction rate constant of (4–9.1) × 10^5 M^{-1} s^{-1} with sulfate radicals and (3.8–7.6) × 10^8 M^{-1} s^{-1} with hydroxyl radicals and preferentially reacts with hydroxyl radicals [66]. The degradation of furfural with and without the quenchers at pH 5.4 and 55 °C is illustrated in Fig. 6a without ferric sulfate and Fig. 6b with ferric sulfate. The molar ratio of furfural to quencher required to observe the quenching at pH 5.4 was 1:100. The change in reaction rate constants in all conditions is shown in Fig. 6c. Without ferric sulfate in solution, methanol quenching caused the reaction rate constant to decrease by 48.5%, while reactions with TBA quenching exhibited a 16.9% decrease in the reaction rate constant. With ferric sulfate in solution, quenching with methanol and TBA impacted the reaction rate constant by causing a 41.5% and 36.3% decrease, respectively. Because the decrease in reaction rate constant is similar for both quenchers when Fe (III) is present, it suggests that hydroxyl radicals play a more prominent role in the degradation process than when Fe (III) is not present in thermally activated persulfate reactions. However, in the absence of Fe (III), sulfate radicals appear to play a more prominent role in the degradation as shown by the increased difference between the reaction rate constants when methanol and TBA are present in solution.

Fig. 7 shows the quenching of the furfural oxidation at pH 2.54, with and without ferric sulfate present. Without ferric sulfate at pH 2.54, methanol quenching decreased the reaction rate constant by 75.4%, while TBA quenched the reaction causing a 64.9% decrease in the observed reaction rate constant as shown in Fig. 7a. With ferric sulfate in solution at pH 2.54, methanol and TBA quenching were similar with an observed decrease of 91.9% and 90.9%, respectively, for the reaction rate constant as displayed in Fig. 7b. Greater decreases in the reaction rate constant were observed as illustrated in Fig. 7c indicating that at pH 2.54, the hydroxyl radical plays a substantial role in furfural degradation via thermal activated persulfate. Moreover, the formation of hydroxyl radicals is even more significant when ferric sulfate is present.

3.6. Intermediate identification and pathway discussion

The transformation byproducts of furfural oxidation via persulfate reaction (55 °C, pH 5.4, 0 mg L^{-1} ferric sulfate, 21 mmol L^{-1} sodium persulfate) were investigated using GC/MS. Mass spectra are provided in Supplementary Materials, Figs. S19–S24. The degradation pathway for furfural oxidation is suggested as shown in Supplementary Materials Fig. S18 based on the reaction byproducts identified in samples taken at different time points in the experiment. Seven products were identified in addition to 3-furaldehyde, including 2-methyl butanoic acid, 3-furancarboxylic acid, 2-ethylpropane-1,3-diol tetrahydrofuran-3-carboxylic acid, (tetrahydrofuran-3-yl)methanol, 2-methylbutanal and tiglic acid. These byproducts indicate that destruction of furfural mainly occurs on the furan ring and the aldehyde functional group of the furfural molecule.

Free radicals attack the nearest stable molecule and generate a radical intermediate or another reaction byproduct [69,70]. When radicals attack furfural, the electrophilic locations, the oxygen of the aromatic ring and the aldehyde functional group, are targeted. Furfural is quickly transformed to furfural radicals through electron transfer from the aromatic ring to the sulfate radicals [71,72]. The resulting furfural radical cation is reactive with the water via hydrolysis, causing opening of the aromatic ring and likely forming 2-ethylmalonaldehyde among other compounds

Table 5
Pseudo first-order reaction rate constants for furfural oxidation via activated persulfate as the iron (III) sulfate concentration increases.

$[Na_2S_2O_8]_i$ (mM)	$[Iron\ Sulfate]_i$ (mg L^{-1})	pH	T (°C)	k_{obs} (s^{-1})	$t_{1/2}$(d)	R^2
15	5	5.4	55	1.30 × 10^{-4}	0.0617	0.93
15	10	5.4	55	1.52 × 10^{-4}	0.0514	0.95
15	25	5.4	55	1.64 × 10^{-4}	0.0489	0.99
15	50	5.4	55	1.40 × 10^{-4}	0.0573	0.99
15	100	5.4	55	8.42 × 10^{-5}	0.0953	0.95

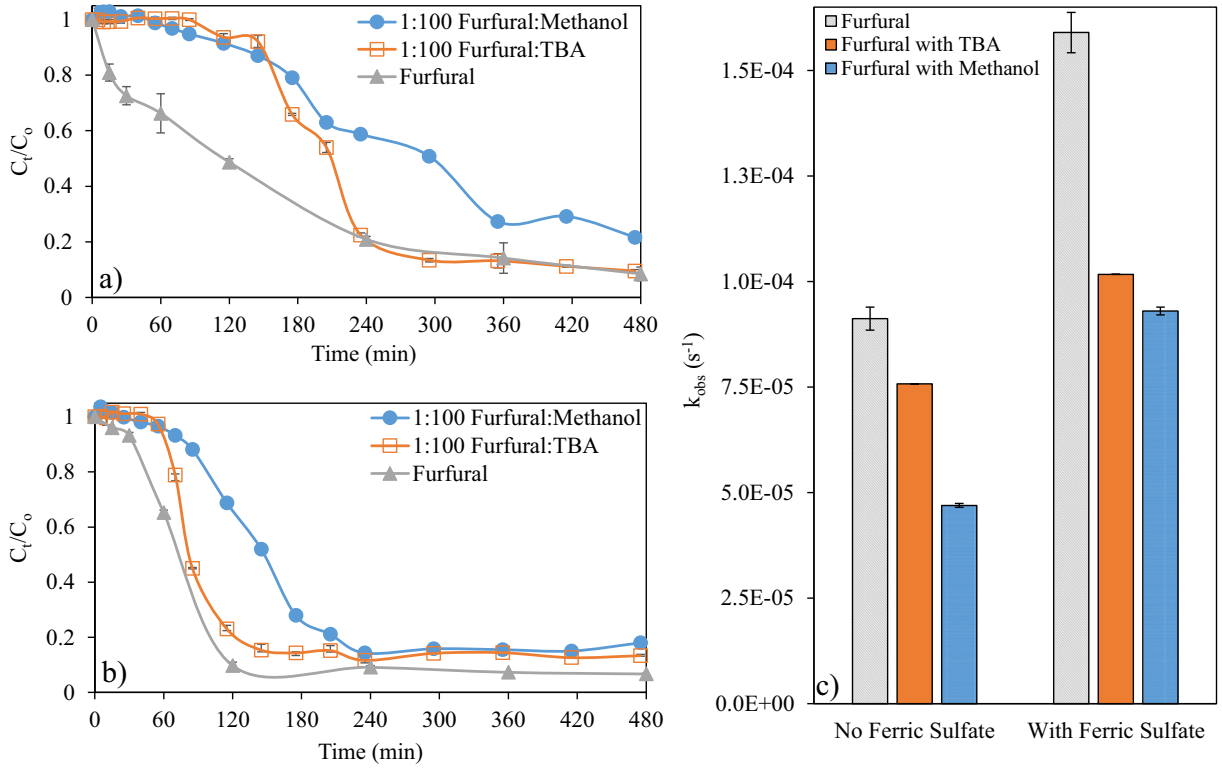

Fig. 6. The degradation of furfural in the presence of quenchers methanol and TBA at 55 °C and pH 5.4 (furfural:quencher = 1:100). Decreasing furfural concentrations are shown in (a) without ferric sulfate and (b) with ferric sulfate. The changes in the observed pseudo first-order reaction rate constants are displayed in (c). For all figures the error bars represent standard error.

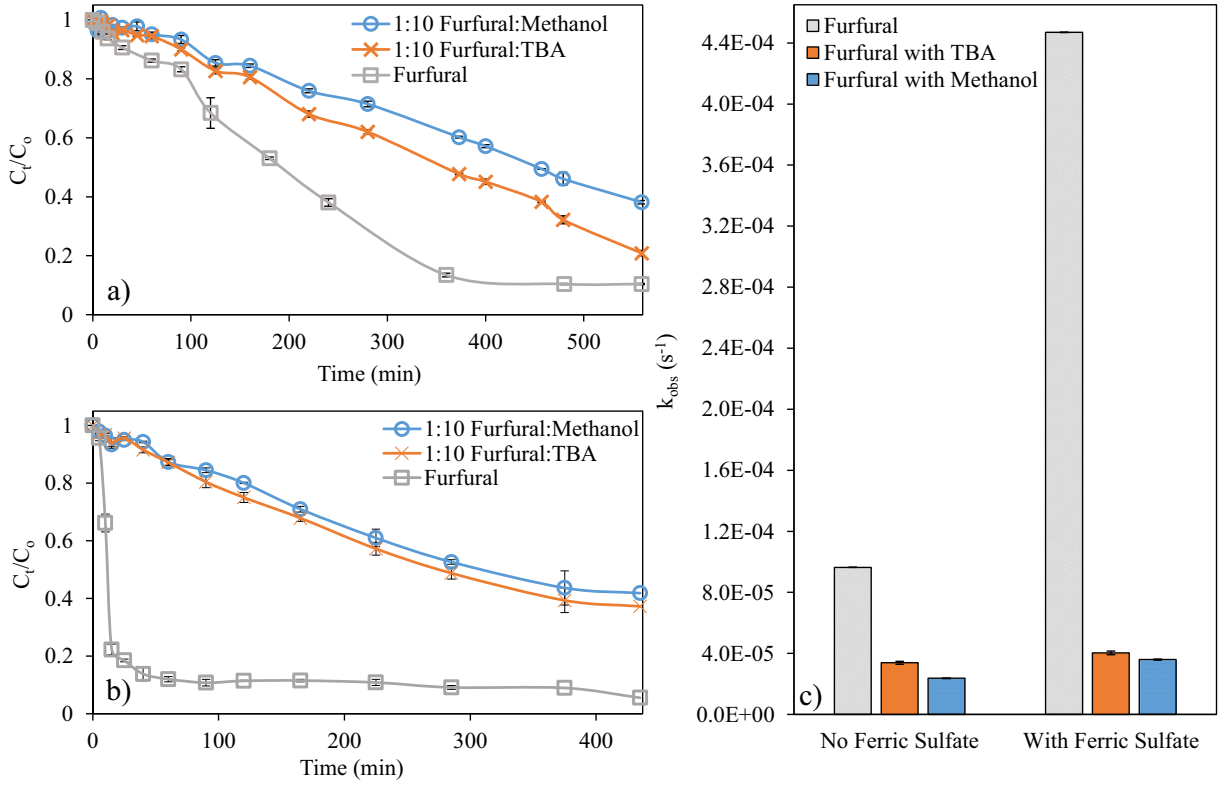

Fig. 7. The degradation of furfural in the presence of methanol and TBA quenchers at 55 °C and pH 2.54 (furfural:quencher = 1:10 M ratio). The decreasing furfural concentrations are shown in (a) without ferric sulfate and (b) with ferric sulfate. The changes in the observed pseudo first-order reaction rate constants are displayed in (c). For all figures the error bars represent standard error.

[73,74]. This intermediate is further oxidized by the acidic conditions to 2-ethylpropane-1,3-diol or further attacked by the radicals in solution. If further attacked, the radical undergoes rearrangement to form the more stable tertiary radical and ultimately forms 2-methylbutanal and tiglic acid as shown in Supplementary Materials Fig. S18. Tiglic acid can undergo hydration since sulfuric acid is likely present to form 2-methyl butanoic acid.

Furfural degradation may also occur because of the increase in acidity as the reaction proceeds [75]. Under acidic conditions, aldehydes may be converted to carboxylic acids. This may cause the faster furfural degradation under acidic conditions as previously discussed. The aldehyde functional group of the furfural molecule may oxidize to the carboxylic acid, furan-3-craboxylic acid, through reaction with the persulfate anion and elimination as shown in Fig. S18. In addition to oxidation, persulfate can degrade contaminants by nucleophilic attack of the sulfate ion on a carbon [76,77]. The hydroxyl and sulfate radical are nucleophilic and may attack the partially positive atoms or groups of atoms in furfural or in its byproducts, which also could have caused the formation of furan-3-craboxylic acid, tetrahydrofurn-3-carboxylic acid, and (tetrahydrofuran-3-yl)methanol.

3.7. GC/MS analysis of LEB-10X

LEB-10X is used as an enzyme-breaking agent by hydraulic fracturing companies. Enzyme breakers, typically consisting of protein molecules, are added to hydraulic fracturing in order to catalyze the breakdown of the polymer gelling agents, thus enabling flow of both the natural gas and the flowback/produced water. Fig. S25 in the Supplementary Materials shows the chromatographic peak of the furfural found in LEB-10X and its mass spectrum. Verification of the furfural peak was performed using a furfural standard. The approximate concentration of LEB-10X added to hydraulic fracturing fluids is 0.025 gallons per 1000 gallons of water. Other compounds identified using NIST11 in LEB-10X were 5-hydroxymethylfurfural, 5-acetoxymethyl-2-furaldehyde, 1-methy l-1H-pyrazole-4-carboxaldehyde, 1-bromo-chloroethane, (E)-1,2-dichloroethylene, 2-fluoro-5-methoxypyrimidine (a cancer drug), chlorozotocin (used in cancer therapy), zearalenone (an estrogenic metabolite), and hemicellulosic compounds glucopyranose, galactapyranose, arbutin, and inositol.

3.8. Furfural degradation in the presence of LEB-10X and WGA

To understand how furfural degradation changes in the presence of hydraulic fracturing chemical additives, decreasing furfural concentrations were traced in solution containing LEB-10X and WGA, a cellulosic gelling agent. Fig. 8a displays the furfural concentration as a function of time in solution containing LEB-10X and WGA in concentrations added by hydraulic fracturing companies and Fig. 8b displays the resulting reaction rate constants (pH 2.54, 23.3 mg L^{-1} ferric sulfate, 21 mmol L^{-1} sodium persulfate). With the addition of just LEB-10X, the furfural degradation rate constant decreased by 50.7%. With the addition of LEB-10X and WGA, the reaction rate constant of furfural decreased by 56.6%. As shown in Fig. S26a in the Supplementary Materials, only 0.68 mmol L^{-1} persulfate remained in all three solutions solution after 120 min. The persulfate was completely depleted by 165 min. While persulfate depletion was observed, furfural concentrations remaining in solution were the same for all the conditions tested. When LEB-10X is present and when it is present with WGA, overall furfural removal in both conditions at 120 min is only 5% different from furfural removal when these additives are not present. Not only did the furfural remain in solution, but the TOC content of all three solutions remained high as seen in Fig. S26b in the Supplementary Materials. With furfural alone, the overall TOC removal is 52.7%. When LEB-10X is added, the overall TOC removal was 32.6%. When WGA is present with LEB-10X, overall TOC removal decreased to 27.3%. This suggests that while the furfural is being degraded to the same extent in all three conditions, the other additives in the gelling agent and the enzyme breaker remain in solution. Rather than breaking down the target gelling agent, persulfate may preferentially break down other components of the fluids in hydraulic fracturing conditions.

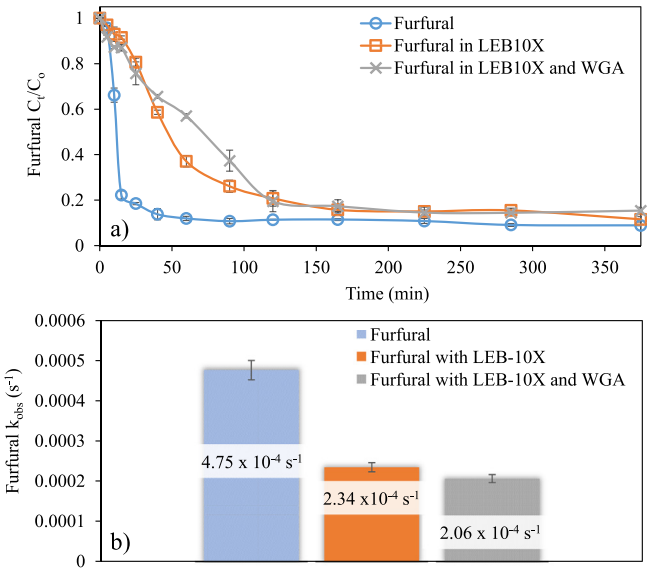

Fig. 8. (a) The decreasing furfural concentrations are shown as a function of time in solution containing Furfural only, Furfural with LEB-10X, and Furfural with LEB-10X and WGA. (b) The resulting reaction rate constants (pH 2.54, 23.3 mg L^{-1} ferric sulfate, 21 mmol L^{-1} sodium persulfate) are displayed for the conditions in (a). All error bars represent standard error.

4. Conclusions

This study investigated the decomposition of furfural, a well-known pollutant in several industries and a chemical component of hydraulic fracturing fluids, via activated persulfate oxidation in water. Furfural degradation was achieved by using radicals, primarily hydroxyl, produced from persulfate activation through heat, pH and iron activation. The mechanism of the furfural/persulfate/Fe (III) reaction without thermal activation (20 °C) warrants further investigation, as both furfural and persulfate were required to initiate iron recycling in this system. Overall, reaction rates were influenced by several different activators, including solution temperature, initial pH, sodium persulfate concentration, and iron concentration. The results indicated that furfural pollution may be oxidized very rapidly via persulfate under hydraulic fracturing conditions. The reaction byproducts were also identified and their transformation mechanisms were suggested. Two chemical additives were used to determine how furfural degradation might change during a fracture. While the presence of the additives did slow down furfural degradation compared to when no additives were present, there was little difference between having LEB-10X, an enzyme breaking agent, in solution and having LEB-10X in solution with WGA, a gelling agent. After 8 h of reacting, furfural was still present in all solutions, which signifies that persulfate may preferentially attack other compounds in the hydraulic fracturing fluids, rather than the target gelling agent. Future studies will investigate the impacts of pressure and hydraulic fracturing brine on the transformation of furfural.

Acknowledgments

Funding for this project was provided by the Science Alliance, A Tennessee Center for Excellence.

Appendix A. Supplementary data

Supplementary data associated with this article can be found, in the online version, at http://dx.doi.org/10.1016/j.cej.2017.06.168.

References

[1] K.B. Gregory, R.D. Vidic, D.A. Dzombak, Water management challenges associated with the production of shale gas by hydraulic fracturing, Elements 7 (2011) 181–186.
[2] A. Vengosh, R.B. Jackson, N. Warner, T.H. Darrah, A. Kondash, A critical review of the risks to water resources from unconventional shale gas development and hydraulic fracturing in the united states, Environ. Sci. Technol. 48 (2014) 8334–8348.
[3] K.E. Carter, R.W. Hammack, J.A. Hakala, Hydraulic Fracturing and Organic Compounds-Uses, Disposal and Challenges, SPE Eastern Regional Meeting, Soc. Petrol. Eng. J. (2013).
[4] R.D. Vidic, S.L. Brantley, J.M. Vandenbossche, D. Yoxtheimer, J.D. Abad, Impact of shale gas development on regional water quality, Science 340 (2013).
[5] W.T. Stringfellow, M.K. Camarillo, J.K. Domen, W.L. Sandelin, C. Varadharajan, P.D. Jordan, M.T. Reagan, H. Cooley, M.G. Heberger, J.T. Birkholzer, Identifying chemicals of concern in hydraulic fracturing fluids used for oil production, Environ. Pollut. 220 (2017) 413–420.
[6] W.T. Stringfellow, J.K. Domen, M.K. Camarillo, W.L. Sandelin, S. Borglin, Physical, chemical, and biological characteristics of compounds used in hydraulic fracturing, J. Hazard. Mater. 275 (2014) 37–54.
[7] E.M. Thurman, I. Ferrer, J. Blotevogel, T. Borch, Analysis of hydraulic fracturing flowback and produced waters using accurate mass: identification of ethoxylated surfactants, Anal. Chem. 86 (2014) 9653–9661.
[8] C.D. Kassotis, D.E. Tillitt, J.W. Davis, A.M. Hormann, S.C. Nagel, Estrogen and androgen receptor activities of hydraulic fracturing chemicals and surface and ground water in a drilling-dense region, Endocrinology 155 (2014) 897–907.
[9] H. Waxman, E. Markey, D. DeGette, Chemicals Used in Hydraulic Fracturing. US House of Representatives Committee on Energy and Commerce Minority Staff, 2013.
[10] E.G. Elliott, A.S. Ettinger, B.P. Leaderer, M.B. Bracken, N.C. Deziel, A systematic evaluation of chemicals in hydraulic-fracturing fluids and wastewater for reproductive and developmental toxicity, J. Expos. Sci. Environ. Epidemiol. 27 (2016) 90–99.
[11] K.E. Manz, K.E. Carter, Extraction and recovery of 2-butoxyethanol from aqueous phases containing high saline concentration, Anal. Chem. Res. 9 (2016) 1–7.
[12] U.S. EPA, Assessment of the Potential Impacts of Hydraulic Fracturing for Oil and Gas on Drinking Water Resources (External Review Draft), in: U.S. EPA (Ed.) Washington, DC, 2015.
[13] M.C. McLaughlin, T. Borch, J. Blotevogel, Spills of hydraulic fracturing chemicals on agricultural topsoil: biodegradation, sorption, and co-contaminant interactions, Environ. Sci. Technol. 50 (2016) 6071–6078.
[14] G.A. Kahrilas, J. Blotevogel, E.R. Corrin, T. Borch, Downhole transformation of the hydraulic fracturing fluid biocide glutaraldehyde: implications for flowback and produced water quality, Environ. Sci. Technol. 50 (2016) 11414–11423.
[15] A.O. Aliu, J. Guo, S. Wang, X. Zhao, Hydraulic fracture fluid for gas reservoirs in petroleum engineering applications using sodium carboxy methyl cellulose as gelling agent, J. Nat. Gas Sci. Eng. 32 (2016) 491–500.
[16] C. Tan, N. Gao, Y. Deng, N. An, J. Deng, Heat-activated persulfate oxidation of diuron in water, Chem. Eng. J. 203 (2012) 294–300.
[17] C.J. Liang, C.J. Bruell, M.C. Marley, K.L. Sperry, Thermally activated persulfate oxidation of trichloroethylene (TCE) and 1, 1, 1-trichloroethane (TCA) in aqueous systems and soil slurries, Soil Sediment Contam. 12 (2003) 207–228.
[18] J. Cooper, L. Stamford, A. Azapagic, Environmental impacts of shale gas in the UK: current situation and future scenarios, Energy Technol. 2 (2014) 1012–1026.
[19] R.C. Navarrete, H.L. Dearing, V.G. Constien, K.M. Marsaglia, J.M. Seheult, P.E. Rodgers, Experiments in fluid loss and formation damage with xanthan-based fluids while drilling, Soc. Petrol. Eng. J (2000).
[20] P.J. Edwards, L.L. Tracy, W.K. Wilson, Chloride concentration gradients in tank-stored hydraulic fracturing fluids following flowback, in: USDA (Ed.), US. Forest Service, Newton Square, PA, 2011.
[21] R.H. Waldemer, P.G. Tratnyek, R.L. Johnson, J.T. Nurmi, Oxidation of chlorinated ethenes by heat-activated persulfate: kinetics and products, Environ. Sci. Technol. 41 (2007) 1010–1015.
[22] I.M. Kolthoff, I.K. Miller, The chemistry of persulfate. I. the kinetics and mechanism of the decomposition of the persulfate ion in aqueous medium, J. Am. Chem. Soc. 73 (1951) 3055–3059.
[23] A. Tsitonaki, B. Petri, M. Crimi, H. MosbÆK, R.L. Siegrist, P.L. Bjerg, In situ chemical oxidation of contaminated soil and groundwater using persulfate: a review, Crit. Rev. Env. Sci. Tech. 40 (2010) 55–91.
[24] G.P. Anipsitakis, D.D. Dionysiou, Transition metal/UV-based advanced oxidation technologies for water decontamination, Appl. Catal., B 54 (2004) 155–163.
[25] S. Yang, P. Wang, X. Yang, L. Shan, W. Zhang, X. Shao, R. Niu, Degradation efficiencies of azo dye Acid Orange 7 by the interaction of heat, UV and anions with common oxidants: Persulfate, peroxymonosulfate and hydrogen peroxide, J. Hazard. Mater. 179 (2010) 552–558.
[26] H. Herrmann, A. Reese, R. Zellner, Time-resolved UV/VIS diode array absorption spectroscopy of SOx−(x = 3, 4, 5) radical anions in aqueous solution, J. Mol. Struct. 348 (1995) 183–186.
[27] P. Neta, V. Madhavan, H. Zemel, R.W. Fessenden, Rate constants and mechanism of reaction of sulfate radical anion with aromatic compounds, J. Am. Chem. Soc. 99 (1977) 163–164.
[28] H. Liu, T.A. Bruton, F.M. Doyle, D.L. Sedlak, In situ chemical oxidation of contaminated groundwater by persulfate: decomposition by Fe(III)- and Mn (IV)-containing oxides and aquifer materials, Environ. Sci. Technol. 48 (2014) 10330–10336.
[29] H. Liu, T.A. Bruton, W. Li, J.V. Buren, C. Prasse, F.M. Doyle, D.L. Sedlak, Oxidation of benzene by persulfate in the presence of Fe(III)- and Mn(IV)-containing oxides: stoichiometric efficiency and transformation products, Environ. Sci. Technol. 50 (2016) 890–898.
[30] Y. Wu, R. Prulho, M. Brigante, W. Dong, K. Hanna, G. Mailhot, Activation of persulfate by Fe(III) species: Implications for 4-tert-butylphenol degradation, J. Hazard. Mater. 322 (Part B) (2017) 380–386.
[31] C. Liang, C.-P. Liang, C.-C. Chen, pH dependence of persulfate activation by EDTA/Fe(III) for degradation of trichloroethylene, J. Contam. Hydrol. 106 (2009) 173–182.
[32] B. Legarth, E. Huenges, G. Zimmermann, Hydraulic fracturing in a sedimentary geothermal reservoir: Results and implications, Int. J. Rock Mech. Min. 42 (2005) 1028–1041.
[33] K. Konschnik, A. Dayalu, Hydraulic fracturing chemicals reporting: Analysis of available data and recommendations for policymakers, Energy Policy 88 (2016) 504–514.
[34] L. Torres, O.P. Yadav, E. Khan, A review on risk assessment techniques for hydraulic fracturing water and produced water management implemented in onshore unconventional oil and gas production, Sci. Total Environ. 539 (2016) 478–493.
[35] V. Marcon, C. Joseph, K.E. Carter, S.W. Hedges, C.L. Lopano, G.D. Guthrie, J.A. Hakala, Experimental insights into geochemical changes in hydraulically fractured Marcellus Shale, Appl. Geochem. 76 (2017) 36–50.
[36] D. Kekacs, M. McHugh, P.J. Mouser, Temporal and thermal changes in density and viscosity of marcellus shale produced waters, J. Environ. Eng. 141 (2015).
[37] I. Ferrer, E.M. Thurman, Chemical constituents and analytical approaches for hydraulic fracturing waters, Trends Environ. Anal. Chem. 5 (2015) 18–25.
[38] E.E. Yost, J. Stanek, R.S. DeWoskin, L.D. Burgoon, Overview of chronic oral toxicity values for chemicals present in hydraulic fracturing fluids, flowback, and produced waters, Environ. Sci. Technol. 50 (2016) 4788–4797.
[39] S. Burden, J. Dean, J. Koplos, C. Meza-Cuadra, A. Singer, M.E. Tuccillo, Analysis of Hydraulic Fracturing Fluid Data from the FracFocus Chemical Disclosure Registry 1, in: U.S. EPA (Ed.), 2015.
[40] FracFocus.org, Chemical Use In Hydraulic Fracturing, (2017) https://fracfocus.org/water-protection/drilling-usage.
[41] E. Barbot, N.S. Vidic, K.B. Gregory, R.D. Vidic, Spatial and temporal correlation of water quality parameters of produced waters from devonian-age shale following hydraulic fracturing, Environ. Sci. Technol. 47 (2013) 2562–2569.
[42] C.G. Struchtemeyer, M.S. Elshahed, Bacterial communities associated with hydraulic fracturing fluids in thermogenic natural gas wells in North Central Texas, USA, FEMS Microbiol. Ecol. 81 (2012) 13–25.
[43] I. Grenthe, W. Stumm, M. Laaksuharju, A.C. Nilsson, P. Wikberg, Redox potentials and redox reactions in deep groundwater systems, Chem. Geol. 98 (1992) 131–150.
[44] E.-L. Tullborg, The influence of recharge water on fissure-filling minerals — A study from Klipperås, southern Sweden, Chem. Geol. 76 (1989) 309–320.
[45] A.D. Webb, G.R. Dickens, N.H.S. Oliver, Carbonate alteration of the upper mount McRae shale beneath the martite-microplaty hematite ore deposit at mount whaleback, Western Australia, Miner. Deposita 39 (2004) 632–645.
[46] A.D. Jew, M.K. Dustin, A.L. Harrison, C.M. Joe-Wong, D.L. Thomas, K. Maher, G.E. Brown, J.R. Bargar, Impact of organics and carbonates on the oxidation and precipitation of iron during hydraulic fracturing of shale, Energy Fuels 31 (2017) 3643–3658.
[47] H.A. Waxman, E.J. Markey, D. DeGette, Chemicals used in hydraulic fracturing, United States House of Representatives Committee on Energy and Commerce Minority Staff (2011).
[48] B.K. Sovacool, Cornucopia or curse? Reviewing the costs and benefits of shale gas hydraulic fracturing (fracking), Renew. Sustainable Energy Rev. 37 (2014) 249–264.
[49] M. Zoveidavianpoor, A. Gharibi, Application of polymers for coating of proppant in hydraulic fracturing of subterraneous formations: A comprehensive review, J. Nat. Gas Sci. Eng. 24 (2015) 197–209.
[50] F. Liang, M. Sayed, G.A. Al-Muntasheri, F.F. Chang, L. Li, A comprehensive review on proppant technologies, Petroleum 2 (2016) 26–39.
[51] A.P. Dunlop, Furfural Formation and Behavior, Ind. Eng. Chem. 40 (1948) 204–209.

[52] D. Kekacs, B.D. Drollette, M. Brooker, D.L. Plata, P.J. Mouser, Aerobic biodegradation of organic compounds in hydraulic fracturing fluids, Biodegradation 26 (2015) 271–287.
[53] M. Leili, G. Moussavi, K. Naddafi, Degradation and mineralization of furfural in aqueous solutions using heterogeneous catalytic ozonation, Desalin. Water Treat. 51 (2013) 6789–6797.
[54] A. Nezamzadeh-Ejhieh, S. Moeinirad, Heterogeneous photocatalytic degradation of furfural using NiS-clinoptilolite zeolite, Desalination 273 (2011) 248–257.
[55] R. Boopathy, H. Bokang, L. Daniels, Biotransformation of furfural and 5-hydroxymethyl furfural by enteric bacteria, J. Ind. Microbiol. Biotechnol. 11 (1993) 147–150.
[56] C. Liang, C.-F. Huang, N. Mohanty, R.M. Kurakalva, A rapid spectrophotometric determination of persulfate anion in ISCO, Chemosphere 73 (2008) 1540–1543.
[57] S.-Y. Oh, H.-W. Kim, J.-M. Park, H.-S. Park, C. Yoon, Oxidation of polyvinyl alcohol by persulfate activated with heat, Fe 2+, and zero-valent iron, J. Hazard. Mater. 168 (2009) 346–351.
[58] K.E. Manz, G. Haerr, J. Lucchesi, K.E. Carter, Adsorption of hydraulic fracturing fluid components 2-butoxyethanol and furfural onto granular activated carbon and shale rock, Chemosphere 164 (2016) 585–592.
[59] C. Liang, Z.-S. Wang, C.J. Bruell, Influence of pH on persulfate oxidation of TCE at ambient temperatures, Chemosphere 66 (2007) 106–113.
[60] K.-C. Huang, R.A. Couttenye, G.E. Hoag, Kinetics of heat-assisted persulfate oxidation of methyl tert-butyl ether MTBE, Chemosphere 49 (2002) 413–420.
[61] S. Rodriguez, L. Vasquez, D. Costa, A. Romero, A. Santos, Oxidation of orange G by persulfate activated by Fe(II), Fe(III) and zero valent iron ZVI, Chemosphere 101 (2014) 86–92.
[62] D. Zhao, X. Liao, X. Yan, S.G. Huling, T. Chai, H. Tao, Effect and mechanism of persulfate activated by different methods for PAHs removal in soil, J. Hazard. Mater. 254–255 (2013) 228–235.
[63] D.A. House, Kinetics and mechanism of oxidations by peroxydisulfate, Chem. Rev. 62 (1962) 185–203.
[64] M.L. Crimi, J. Taylor, Experimental evaluation of catalyzed hydrogen peroxide and sodium persulfate for destruction of BTEX contaminants, Soil Sediment Contam. 16 (2007) 29–45.
[65] I. Kolthoff, A. Medalia, H.P. Raaen, The reaction between ferrous iron and peroxides. IV. Reaction with potassium persulfate, J. Am. Chem. Soc. 73 (1951) 1733–1739.
[66] C. Liang, H.-W. Su, Identification of sulfate and hydroxyl radicals in thermally activated persulfate, Ind. Eng. Chem. Res. 48 (2009) 5558–5562.
[67] I. Hussain, Y. Zhang, S. Huang, Q. Gao, Degradation of p-chloroaniline by FeO 3− x H 3–2x/Fe 0 in the presence of persulfate in aqueous solution, RSC Adv. 5 (2015) 41079–41087.
[68] X. Li, W. Guo, Z. Liu, R. Wang, H. Liu, Fe-based MOFs for efficient adsorption and degradation of acid orange 7 in aqueous solution via persulfate activation, Appl. Surf. Sci. 369 (2016) 130–136.
[69] S.A. Bhange, D.V. Parwate, P.S. Kolte, Corollary of additives on gamma and pulse radiolytic degradation of aqueous potassium permanganate solution, Anal. Chem. Lett. 3 (2013) 264–270.
[70] S.-C. Hsu, T.-M. Don, W.-Y. Chiu, Free radical degradation of chitosan with potassium persulfate, Polym. Degrad. Stab. 75 (2002) 73–83.
[71] G.P. Anipsitakis, D.D. Dionysiou, M.A. Gonzalez, Cobalt-mediated activation of peroxymonosulfate and sulfate radical attack on phenolic compounds. Implications of chloride ions, Environ. Sci. Technol. 40 (2006) 1000–1007.
[72] C. Minero, G. Mariella, V. Maurino, E. Pelizzetti, Photocatalytic transformation of organic compounds in the presence of inorganic anions. 1. Hydroxyl-mediated and direct electron-transfer reactions of phenol on a titanium dioxide−fluoride system, Langmuir 16 (2000) 2632–2641.
[73] G. Mengoli, M.M. Musiani, M. Fleischmann, D. Pletcher, Studies of pyrrole black electrodes as possible battery positive electrodes, J. Appl. Electrochem. 14 (1984) 285–291.
[74] C. Tan, N. Gao, W. Chu, C. Li, M.R. Templeton, Degradation of diuron by persulfate activated with ferrous ion, Sep. Purif. Technol. 95 (2012) 44–48.
[75] J. Lee, B. Uff, Organic reactions involving electrophilic oxygen, Q. Rev. Chem. Soc. 21 (1967) 429–457.
[76] R.S. Varma, H.M. Meshram, Solid state cleavage of semicarbazones and phenylhydrazones with ammonium persulfate-clay using microwave or ultrasonic irradiation, Tetrahedron Lett. 38 (1997) 7973–7976.
[77] J.A. Ashenhurst, Intermolecular oxidative cross-coupling of arenes, Chem. Soc. Rev. 39 (2010) 540–548.